UNIVERSITY OF BUCHAREST

FACULTY OF CHEMISTRY

DOCTORAL THESIS

Experimental and theoretical study of some molecular interactions

- SUMMARY -

Doctoral advisor,

Prof. dr. Mihaela Hillebrand

Ph. D. student,

Sandu Romică

2012

CONTENTS*

** The numbering of chapters, figures and tables is that presented in the thesis.

INTRODUCTION

The thesis is structured in two parts: The Theoretical Part, presented in three chapters, and The Original Part, conducted over four chapters, which present the results of the original studies performed. The first chapter and the second provide a description of the studied ligand-macromolecule systems and the thermodynamics of the occurring interactions.

As part of the third chapter, in the first two subchapters are presented experimental techniques used in this study: isothermal titration calorimetry and circular dichroism spectroscopy. In the last subchapter are presented theoretical methods applied to modeling of ligands and inclusion complexes.

ORIGINAL RESULTS

The PhD thesis has the following objectives presented in the four chapters of the original part:

1) Characterization by circular dichroism spectroscopy of the interaction of phenoxathiin derivatives with cyclodextrins; theoretical modeling of the ligands by DFT and TDDFT methods; theoretical modeling of the inclusion complexes by molecular dynamics simulation.
2) Characterization by isothermal titration calorimetry of the interaction of coumarin derivatives, phenoxathiin and atenolol with cyclodextrins.
3) Characterization by isothermal titration calorimetry of the interaction of coumarin derivatives with human serum albumin.

The thesis ends with the conclusions chapter that contains the main results obtained, followed by a list of papers resulting from the thesis, the bibliography used and annexes. The annexes include tables and figures that are mentioned in the text of the thesis.

PART II (original results)

Chapter 4

EXPERIMENTAL METHODS USED IN THE STUDY OF LIGAND-CYCLODEXTRIN AND LIGAND-ALBUMIN INTERACTIONS

4.1 ISOTHERMAL TITRATION CALORIMETRY

The titration experiments were performed using an iTC200 microcalorimeter (MicroCal Inc., Northampton, MA, USA). This calorimeter is of power compensation type and is designed to work with small volumes of solutions [31]. The sample cell was filled with 280 μL of titrate solution and the syringe was filled with 40 μL of titrant solution. The samples were degassed under vacuum, prior to using for ITC runs. The reference cell was filled with deionized and degassed water [33].

4.2 CIRCULAR DICHROISM SPECTROSCOPY

Induced circular dichroism (ICD) spectra were recorded at room temperature with a spectrophotometer Jasco J-815 CD.

The binding constants for the complexes with CyD, K, were estimated using linear and nonlinear regression models for a complex with 1:1 stoichiometry, in terms of $\Delta\theta$, the difference between experimental ellipticities of the guest in the absence and presence of CyD read at a definite wavelength and the total molar concentrations of the guest and the cyclodextrins, [G] and [CyD], respectively.

The linear model is based on eq. (15) known as the Scott [44] equation:

$$\frac{[G][CyD]d}{\Delta\theta} = \frac{[CyD]}{\Delta\psi} + \frac{1}{K\Delta\psi} \tag{15}$$

where $\Delta\psi$ represents the difference in the molar ellipticity coefficient between the complexed and free guest and d is the path-length of the cell.

The non linear model described by Zsila *et al*. [44] corresponds to eq. (16)

$$\Delta\theta = \frac{k}{2}\left([CyD]+[G]+K^{-1} - \sqrt{\left([CyD]+[G]+K^{-1}\right)^2 - 4\times[CyD]\times[G]}\right) \tag{16}$$

where $\Delta\theta$ and K have the same meaning as in eq. (15) and k is correlated with the dichroic signal at total complexation.

4.3 THEORETICAL MODELING OF THE LIGAND-CYCLODEXTRIN INTERACTION

4.3.1 THE MODELING OF LIGANDS BY DFT AND TDDFT METHODS

The lowest energy geometries and ligand structure were obtained by the DFT method using the Gaussian03 program [56], with the functionals B3LYP and PBE in conjunction with the 6-31G [57], 6-311G++(d,p) [58] and aug-cc-pVDZ [59] basis sets. The optimisations were performed considering the solvent, water, in the frame of the Polarisable Continuum Model, PCM [60]. The MO calculations were performed by DFT and TDDFT methods considering different possible conformers characterized by the dihedral angle τ describing the position of substituents in respect to the heteroring.

4.3.2 THE MOLECULAR DYNAMICS SIMULATIONS OF THE INCLUSION COMPLEXES

The molecular dynamics simulation was performed using Gromacs software package. The initial structure for the CyD-ligand 2:1 complex was obtained by docking with Autodock. The force field used was OPLSAA (Optimized Potential for Liquid Simulations - All Atoms), the partial atomic charges calculated by Gasteiger method. In the simulation all atoms and water molecules are treated explicitly. Trajectory was collected over 2000 ps and the balanced structure of the complex solvated in a final trajectory of 1000 ps was extracted.

Chapter 5

THE STUDY OF LIGAND-CYCLODEXTRIN INTERACTIONS BY CIRCULAR DICHROISM SPECTROSCOPY

In this chapter is presented a comparative study of the process of inclusion of three derivatives from the phenoxathiin class, **10,10-dioxide-phenoxathiin**, the 2-bromomethyl substituted derivative, **CH_2Br-10,10-dioxide-phenoxathiin**, and the 2-$COCH_3$ substituted derivative, **2-acetyl-10,10-dioxide-phenoxathiin**, with α -, β -, - γ and 2-hydroxypropyl-γ-cyclodextrin, using as experimental method the circular dichroism spectroscopy. First, host concentration dependence of the induced dichroic signal was analyzed in terms of a nonlinear model that allows estimation of the

stoichiometry and association constants of the complex. Then, the sign of the induced dichroic bands in conjunction with the TDDFT calculations of polarization of electronic transitions were used to determine the axial or equatorial guest inclusion mode into the host cavity.

5.1 Experimental data

5.1.2 MATERIALS AND METHODS

10,10-dioxide-phenoxathiin was purchased from Aldrich and 2-acetyl-10,10-dioxide-phenoxathiin and 2-brommethyl-10,10-dioxide-phenoxathiin were synthesized as previously described [95]. β- and γ-CyD were purchased from Aldrich and 2-hydroxypropyl-γ-CyD (2-HP-γ-CyD) was a gift from Prof. Szejtli (CycloLab). The solutions were prepared using a stock solution of approximately 10^{-4} M phenoxathiin derivative in methanol:water (1:9 v/v) to which CyD solution was added. The phenoxathiin concentration was kept constant. The circular dichroism spectra were recorded on JASCO J-815-CD spectrometer under the conditions: 1 nm bandwidth, response time of 8 s, scan speed of 50 nm/min, the number of accumulations 5.

5.1.3 RESULTS AND DISCUSSION

10,10-dioxide-phenoxathiin (Phx-SO_2)

Electronic absorption spectrum of Phx-SO_2 in water is shown in Fig. 10.

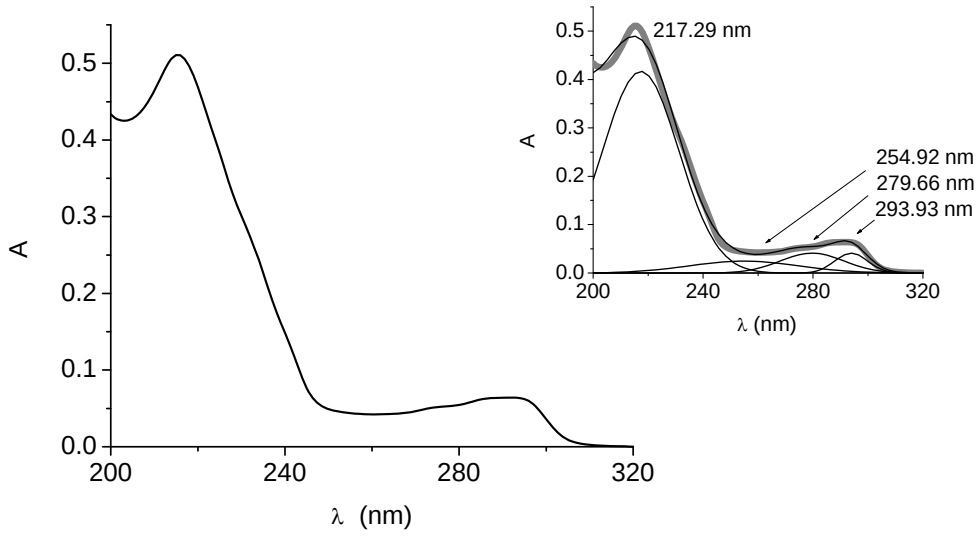

Fig. 10 Absorption spectra of Phx-SO_2 and its respective deconvolution (insets, experimental spectra in gray).

Phx-SO_2 presents in the electronic absorption spectrum a broad band, not very intense, in the range 290-270 nm and a second intense band at 220 nm. UV spectrum deconvolution (Fig. 10) shows that the first band actually consists of three overlapping bands with peaks at 293.93, 279.66 and 254.92 nm.

Phx-SO_2 free in solution has no dichroic signal. However, in the presence of β-, γ - and 2-HP-γ-Cyd was recorded a complex dichroic signal generated by ligand confinement inside the CyD cavity and the asymmetry of the latter, and attesting the occurrence of the inclusion process. As an example, the ICD spectra obtained in the presence of β-CyD are shown in Fig. 11. In the case of α-CyD, the cyclodextrin with the smallest cavity, the ICD signal recorded was very low and will not be considered further. The association constants were estimated using a nonlinear model characterized by Eq. 16 [44]. The best fitting obtained for Phx-SO_2 are shown in Fig. 14 using the experimental values at 267 nm and 218 nm. The results show the formation of 1:1 complexes. The association constants obtained for the interaction of Phx-SO_2 with β-, γ - and 2-HP-γ-CyD are included in Tab. 3.

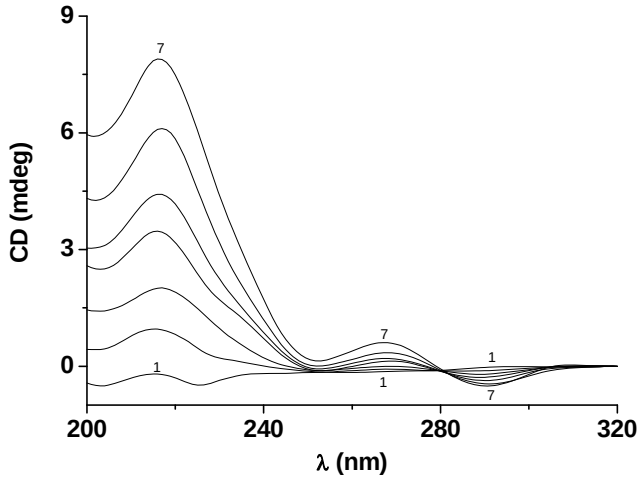

Fig. 11 ICD spectra of Phx-SO_2 in the presence of increasing concentrations of β-CyD: (A): 1) 0.0 M, 2) 2.41×10^{-4} M, 3) 5.57×10^{-4} M, 4) 1.07×10^{-3} M, 5) 1.49×10^{-3} M, 6) 2.27×10^{-3} M, 7) 4.57×10^{-3} M. [Phx-SO_2] = 4.15×10^{-5} M.

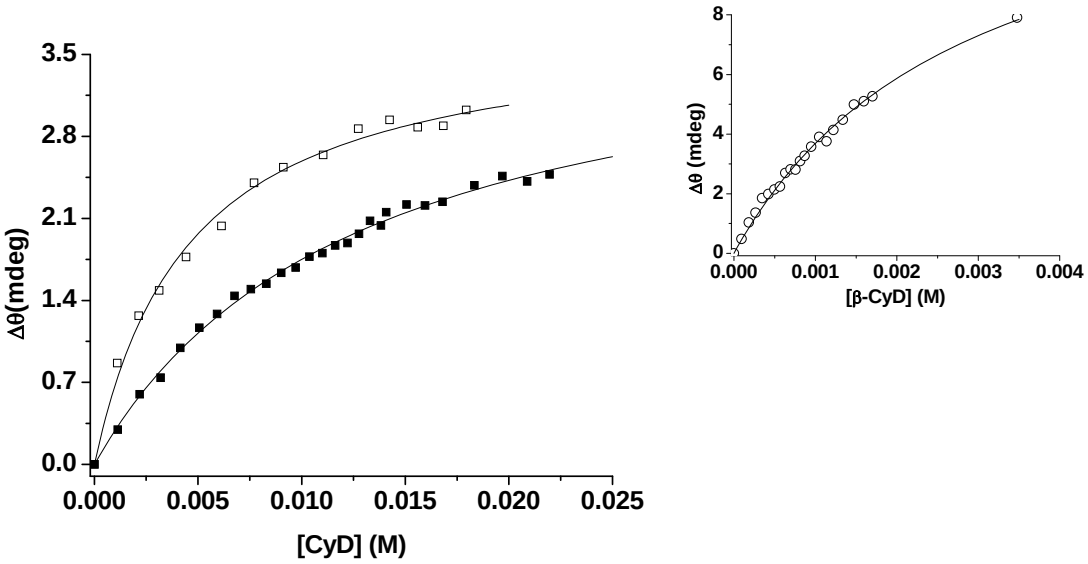

Fig. 14 Best fits obtained for the 1:1 inclusion complexes of Phx-SO_2 with γ-CyD (▫) and 2-HP-γ-CyD (▪) using a nonlinear model (experimental readings at 267 nm). Inset: best fit obtained for the 1:1 complex of Phx-SO_2 with β-CyD (∘) (experimental readings at 218 nm).

Tab. 3 Association constants (K) of Phx-SO_2 with β-, γ- and 2-HP-γ-CyD. r^2-correlation coefficient

CyD	Phx-SO_2	
	K (M^{-1})	r^2
β	357 ± 28	0.991
γ	223 ± 17	0.993
2-HP-γ	80 ± 4	0.997

The data in Tab. 3 shows that for the unsubstituted phenoxathiinsulphone, the association constant decreases from β-CyD to γ- and 2-HP-γ-CyD, the cyclodextrins with larger cavity.

2-bromomethyl-10,10-dioxide-phenoxathiin (Phx-SO_2-CH_2Br)

The electronic absorption spectra of Phx-SO_2-CH_2Br in water shows that both the substituent and/or the substituted position perturb only slightly the electronic system of the heteroring. As with Phx-SO_2, the free compound in solution gives no dichroic signal, due to rapid mediation to zero of heteroring flip-flap motion. In the case of the compound Phx-SO_2-CH_2Br, the lack of a dichroic signal also reflects the free rotation of the group. These experimental observations will be correlated with theoretical calculations. In the presence of β-, γ- and 2-HP-γ-CyD was recorded a complex dichroic signal. ICD spectra obtained in the presence of β-CyD are shown in Figure 16. For α-CyD, the cyclodextrin with the smallest cavity, the ICD signal recorded was very low and will not be considered further. Results show the formation of 1:1 complexes. Association constants are listed in Tab. 4.

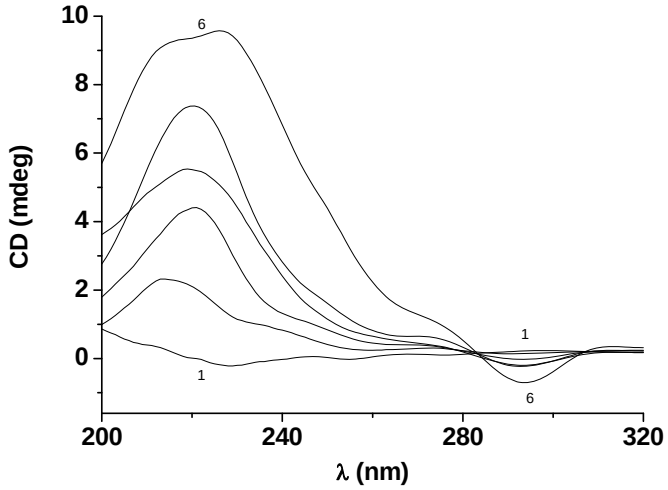

Fig. 16 ICD spectra of Phx-SO_2-CH_2Br in the presence of increasing concentrations of β-CyD: 1) 0.0 M, 2) 1.42×10^{-4} M, 3) 4.05×10^{-4} M, 4) 7.52×10^{-3} M, 5) 1.05×10^{-4} M, 6) 5.26×10^{-3} M. [Phx-SO_2-CH_2Br] = 7.36×10^{-5} M.

Tab. 4 Association constants (K) of Phx-SO_2-CH_2Br with β-, γ- and 2-HP-γ-CyD. r^2-correlation coefficient

CyD	Phx-SO_2-CH_2Br	
	K (M^{-1})	r^2
β	363 ± 25	0.994
γ	113 ± 5	0.996
2-HP-γ	198 ± 26	0.987

The data in Tab. 4 shows the following. The association constant of Phx-SO_2-CH_2Br in the presence of β-CyD is quite similar to that of Phx-SO_2, while a inversion of the values was obtained for the other two cyclodextrins, i.e. a higher value for the interaction with 2-HP-γ-CyD compared to that with γ-CyD.

2-acetyl-10,10-dioxide-phenoxathiin (Phx-SO_2-$COCH_3$)

Induced circular dichroism spectra of Phx-SO_2-$COCH_3$ in the presence of increasing concentrations of β-CyD is given in Fig. 20. At gradual increase of β-CyD, two positive bands at 280 nm and 259-262 nm are apparent, the latter being more intense. Dichroic bands were obtained for all the three CyDs used, but the main features of the bands were somewhat different, likely reflecting the effect of the cavity dimensions. The ICD spectra recorded for similar concentrations of the three CyDs are presented in Fig. 21. It can be seen that in the presence of 2HP-β-CyD, the ICD spectrum is characterized by the two positive bands, as previously discussed for β-CyD. However, at the same concentration of CyDs, the relative intensities of these two bands are different. In the presence of 2HP-β-CyD only the band at 262 nm has a significant intensity, the other band being observed merely as a shoulder. In the same time, a very low intensity signal is evidenced around 300 nm. A deconvolution of the ICD spectrum (Fig. 21, inset) leads to the exact positions of the three bands at 260 nm, 284 nm and 309 nm.

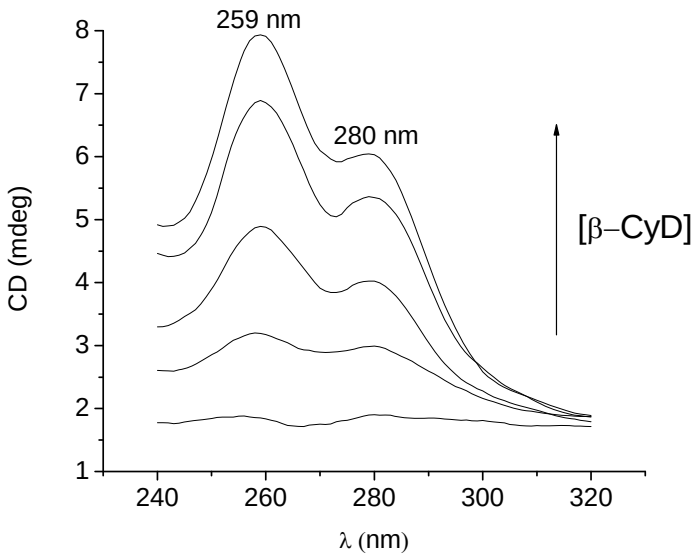

Fig. 20 Induced circular dichroism spectra of Phx-SO_2-$COCH_3$ in the presence of increasing concentrations of β-CyD.

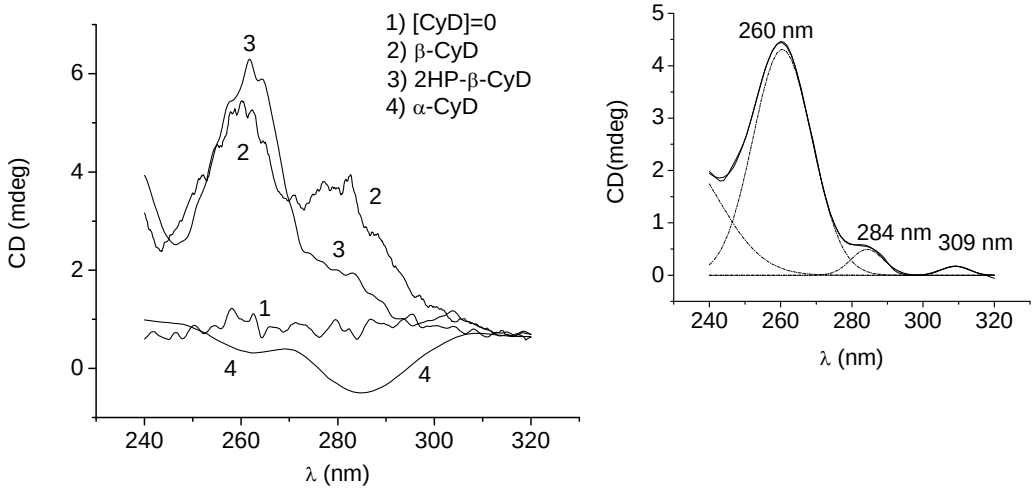

Fig. 21 Induced circular dichroism bands of Phx-SO_2-$COCH_3$ in the absence (1) and in the presence of equal concentrations of CyDs (2, 3, 4). Inset: deconvolution of the smoothed ICD spectrum recorded in the presence of 2HP-β-CyD.

In the case of α-CyD, both main ICD bands are evidenced but with a negative sign, and different relative intensities, the band at 285 nm being the most intense. The binding constants for the complexes with β- and 2HP-β-CyD, K, enumerated în Tab. 5, were estimated using linear and nonlinear regression models [43, 44, 100-104], for a complex with 1:1 stoichiometry.

Tab. 5 Association constants of Phx-SO_2-$COCH_3$, K (M^{-1}), obtained by fitting the experimental data to eqs. (15) and (16) and r the correlation coefficient of the fit.

CyD	β-CyD		2HP-β-CyD	
Model	Eq. 15	Eq. 16	Eq. 15	Eq. 16
K	276.2	260.4	588.1	569.3
r	0.976	0.986	0.972	0.977

The binding constant for the inclusion complex in α-CyD was not estimated due to the low variation in the ellipticities with the CyD concentration and the uncertainty in the complex stoichiometry.

5.2 Theoretical modeling of the ligands at DFT level. Induced dichroism spectrum simulation by the TDDFT method.

In this subchapter is presented a comparative study of the three derivatives from the phenoxathiin class, **10,10-dioxide-phenoxathiin** (Phx-SO_2), the derivative CH_2Br 2-substituted, **2-bromomethyl-10,10-dioxide-phenoxathiin** (Phx-SO_2-CH_2Br), and the derivative 2-$COCH_3$ substituted, **2-acetyl-10,10-dioxide-phenoxathiin** (Phx-SO_2-$COCH_3$), using as a method the theoretical modeling and simulation of absorption spectra and circular dichroism at DFT and TDDFT level.

The experimental data are rationalized in terms of the TDDFT results considering three conformational models of ligand: two roof-shaped models, concave (I) and convex (II) shown in Fig. 24, and a completely flat model. Regarding the CH_2Br and $COCH_3$ substituents, calculations were performed varying the angle τ (Fig. 24), in the range 0-360 degrees, i.e. assuming full rotation of the groups.

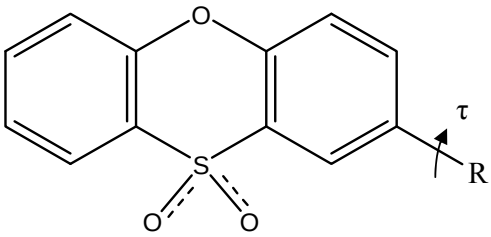

R=H Phx-SO_2

R=CH_2Br Phx-SO_2-CH_2Br

R= $COCH_3$ Phx-SO_2- $COCH_3$

I **II**

Fig. 24 The structure of the guests; the two possible roof-shaped conformations of the heteroring, concave and convex, are denoted by **I** and **II**, respectively; τ represents the torsion of the CH_2Br and $COCH_3$ groups in respect with the heteroring.

The calculated polarization of the electronic transitions in connection with the experimental data permits the establishment of the mode of inclusion of the compound in the CyD cavity.

5.2.2 RESULTS AND DISCUSSION

10,10-dioxide-phenoxathiin

Given the three models already mentioned for the structure of the heteroring, an estimation of the energy barrier to inversion was taken as the difference between the completely flat and one roof-shaped structures.

The values obtained (Tab. 7) were 0.53 kcal mol^{-1} with basic set 6-31G(d) and 0.11 kcal mol^{-1} using the larger basic set 6-311++G(d, p). Using both basic sets, the ECD spectra calculated for the roof-shaped conformations present an object-mirror

image relationship to each other, as shown in Fig. 25 for the 6-31G basis set. The signals are of low intensity, the highest being in the range 220-230 nm, where MO calculations predict transitions involving mainly-phenyl cycle related MO.

Tab. 7 Total energies (ha) for the concave roof-shaped and planar conformations of Phx-SO_2 and the barrier to inversion, ΔE (kcal mol^{-1}).

Atomic basis set	Energy (Ha)		$\Delta E = E_{pl} - E_{\mathbf{I}}$ (kcal mol^{-1})
	Conformation **I**	Planar conformation	
6-31G(d)	-1085.8831888	-1085.8823479	0.53
6-311++G(d,p)	-1086.1061656	-1086.1059956	0.11

Although the frozen conformations are chiral, the small values of the barrier between the two enantiomers support the experimental observation on the achirality of phenoxathiinsulphone in solution. The polarizations of the electronic transitions I, II, IV and V are displayed in Fig. 26.

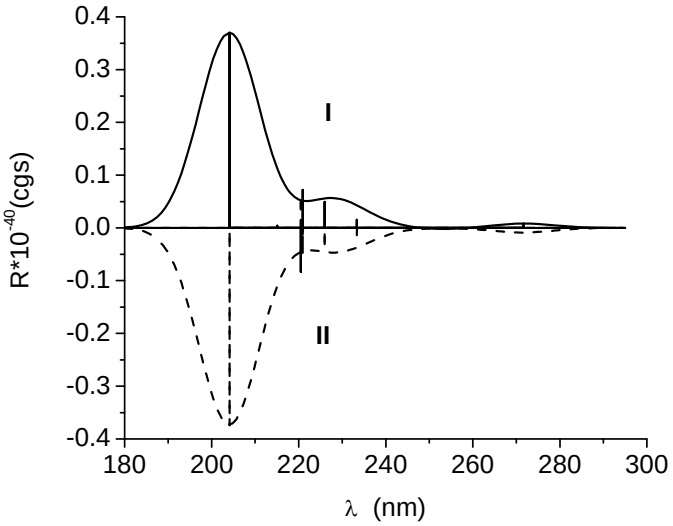

Fig. 25 Calculated (B3LYP/6-31G(d)) ECD spectra for conformations **I** and **II** of Phx-SO_2.

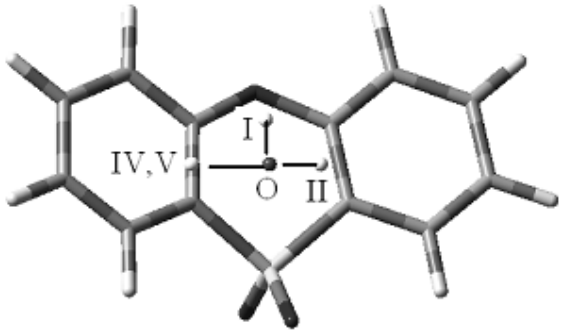

Fig. 26 Direction of the transition moments for the main electronic transitions of Phx-SO_2 (B3LYP/6-31G(d)); O - the origin of the system; I, II, IV, V - the transitions with significant f value.

The comparison of the experimental and theoretical electronic spectra allows for the following remarks. The positions of the two bands in the longest wavelength region are predicted at slightly lower values than the experimental ones, the most intense one being calculated at 272 nm (6-31G(d) basis) and 280 nm (6-311++G(d,p) basis) instead of 290 nm. The relative intensities of the two groups of bands (225 nm *vs*. 260 nm) are correctly predicted.

By correlating the signs of the induced dichroic bands and the directions of the transition moments, the Kodaka-Harata rules reflect an axial inclusion of the guest in the CyD cavity. The polarization of the first electronic transition (272 nm) is orthogonal to the long molecular axis while the three other transitions (254, 226 and 221 nm, II, IV and V) are polarized along the major molecular axis, accounting for the sequence of signs –, +, +, + of the ICD signal.

2-bromomethyl-10,10-dioxide-phenoxathiin

This compound (Phx-SO_2-CH_2Br) presents two possible chiral elements: the flip-flap motion of the rings and the rotation of the substituent.

The potential energy curve for the B3LYP/6-31G calculation is presented in Fig. 28. The minimum energy points were found at ± 90 deg, at full optimization the value being –92.7 deg. Estimating the energy barrier as the difference between the values at τ = 180 deg and τ = 90 deg, we obtain 3.33 kcal mol^{-1}. Using the larger basis, the barrier to rotation was somewhat larger, 3.92 kcal mol^{-1} (Tab. 8).

The potential energy curve in respect to the torsion of the substituent to the ring (τ in Fig. 24) was built for fixed values of τ (0<τ<360 deg with a step of 30 deg) and allowing for the relaxation of all the other internal coordinates.

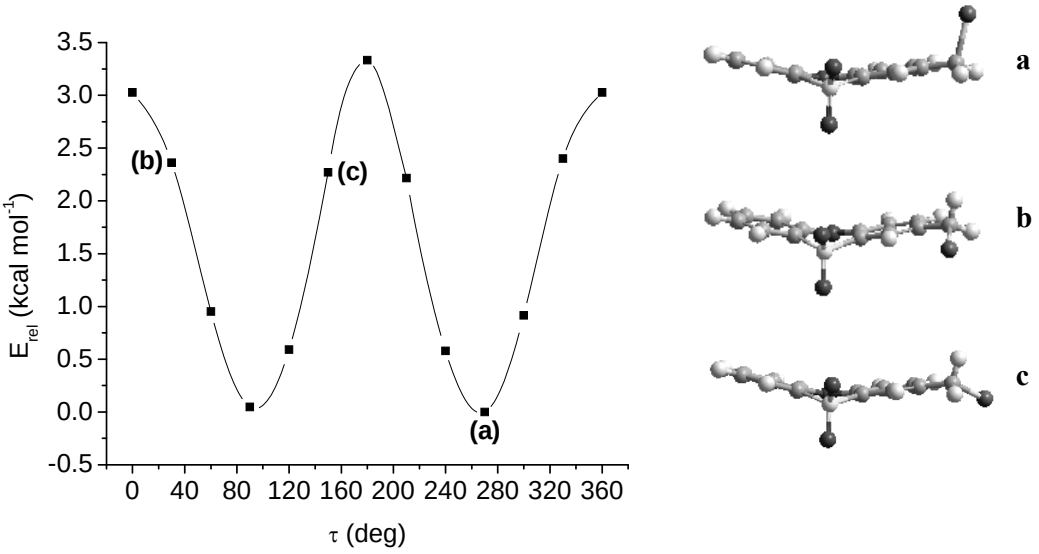

Fig. 28 Potential energy curve built in respect to the torsion angle τ of the CH_2Br group, considering conformation **I** of the heteroring (B3LYP/6-31G(d)).

Tab. 8 Total energies (Ha) of Phx-SO_2-CH_2Br for the conformations used for estimating the barrier to rotation of the CH_2Br group, ΔE (kcal mol^{-1})

Atomic basis set	Energy (Ha)		$\Delta E = E_{\tau=180} - E_{\tau=-90}$
	τ = -90°	τ = -180°	(kcal mol^{-1})
6-31G(d)	-3696.0036200	-3695.99830000	3.34
6-311++G(d,p)	-3698.9793045	-3698.97305924	3.92

We can therefore assume that in the absence of CyD, the group is freely rotating, meaning achiral properties. The small values of the calculated energy barrier for both processes show that in solution all conformations are possible, conferring to the molecule the observed achirality. However, we have found that the calculations were very sensitive to the position of the bromine atom in respect to the SO_2 group and the shape of the heteroring. The plot of the simulated ECD spectra for the three conformers is given in Fig. 29.

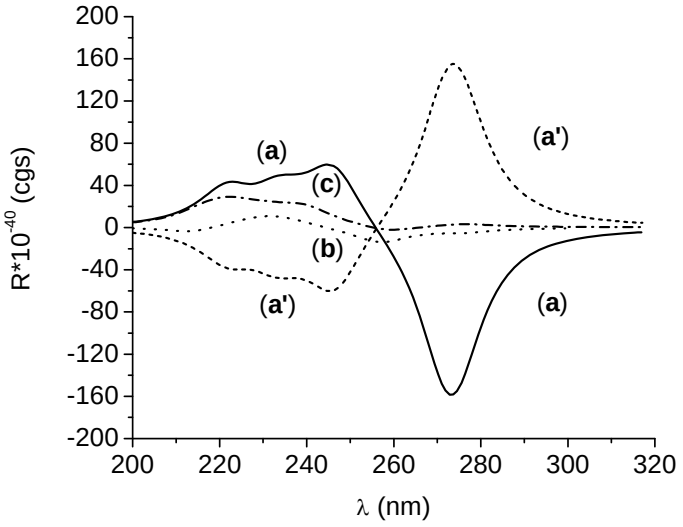

Fig. 29 Calculated ECD spectra (B3LYP/6-31G(d)) for Phx-SO_2-CH_2Br; **a**, **b**, **c** - conformers presented in Fig. 9, differing by the position of the CH_2Br group (conformation **I** of the heteroring); **a'**- enantiomer of **a**, conformation **II**.

The calculated electronic spectrum of Phx-SO_2-CH_2Br is similar with that of the unsubstituted compound, supporting the experimental observation on the slight influence produced by the substituent on the overall system. The transition moments of the main transitions for these conformers are plotted in Fig. 31.

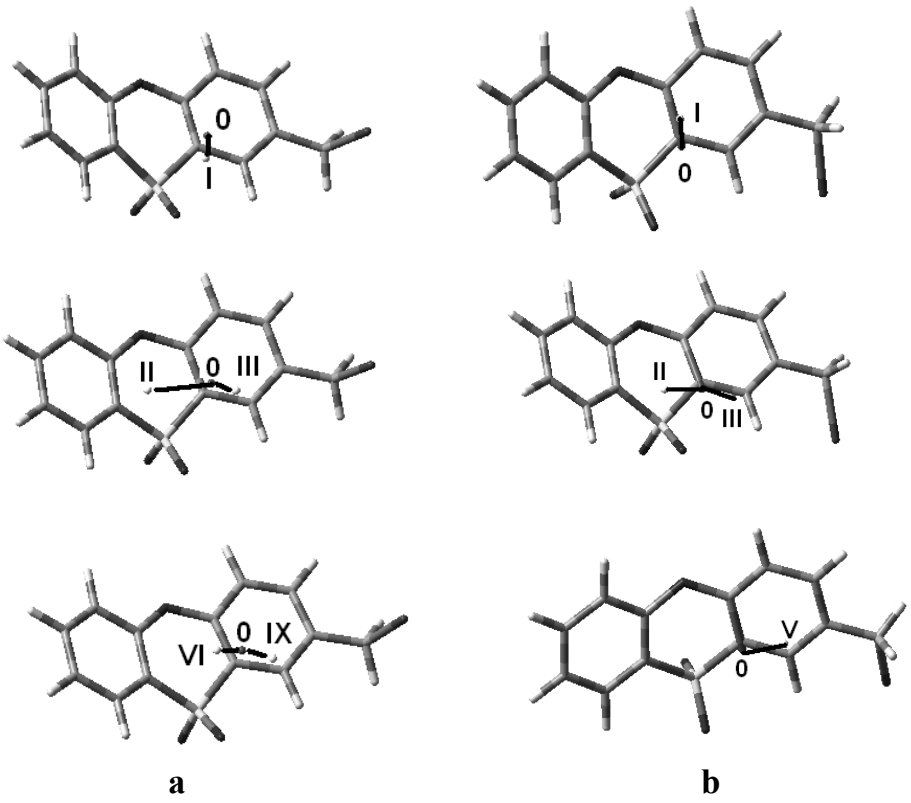

Fig. 31 Direction of the transition moments for the main electronic transitions of Phx-SO_2-CH_2Br (B3LYP/6-31G(d)), conformers **a** and **b**; O - the origin of the system; I-IX - the transitions with significant f value.

For both conformers, the first transition, although assigned to different MOs, is polarized along the short molecular axis. As concerns the other transitions, the most intense, they are polarized parallel to the long molecular axis. Therefore, the correlation of the Harata-Kodaka rules with the TDDFT results on the directions of the transition moments allows for considering that both molecules are included in the CyD cavities in an axial mode.

2-acetyl-10.10-dioxide-phenoxathiin

The electronic transitions for Phx-SO_2-$COCH_3$ were calculated for several conformers characterized by different τ values. τ was varied with a step of 30° in the

range of 0° –180°. The experimental spectrum and the calculated ones for the planar, τ = 0°, and twisted, τ = 90°, conformers are displayed in Fig. 32.

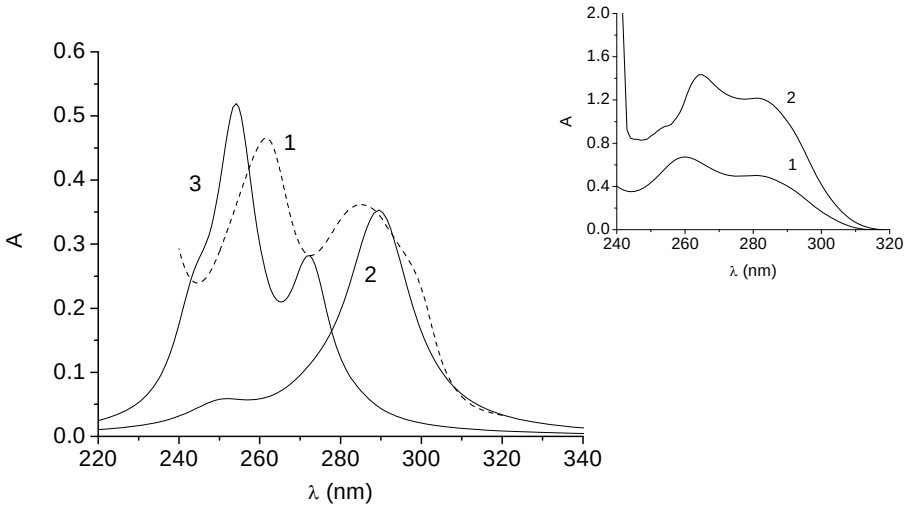

Fig. 32 Experimental and calculated TDDFT (B3LYP/6-31G) absorption spectra of Phx-SO_2-$COCH_3$: 1)-experimental; 2) calculated, τ = 0°; 3) calculated, τ = 90°. Inset: experimental spectra in methanol (1) and ethylene glycol (2)

Some relevant results are listed in Tab. 9 and the directions of the transitions moments for the most intense (f > 0.0030) electronic bands in the range 230-350 nm are displayed in Fig. 33 for three conformers (τ: 0°; 60°; 90°).

The comparison of the spectra in Fig. 32 leads to the following observations. Although the predicted positions of the bands correspond in a satisfactory manner with the experimental spectrum, the latter is wider than the calculated spectra, presumably reflecting the presence in solution of different conformers.

Tab. 9

Wavelengths (λ), oscillator strengths (f) and assignment (*h* = *homo*; *l* = *lumo*) of the electronic absorption bands calculated at the B3LYP/6-31G level for the totally planar, τ=0° and 180° and twisted conformers, τ=90°

τ	0°; 180°;			τ	90°		
E	–1238.5291566 Ha ; –1238.5294281Ha			E	–1238.51806 Ha		
Nr	λ (nm)	f	Assignment	Nr	λ (nm)	f	Assignment
1	324.99	0.0002	$h\text{-}1 \rightarrow l$	1	286.43	0.0021	$h\text{-}1 \rightarrow l\text{+}2$
2	289.51	0.3448	$h \rightarrow l$	2	273.57	0.0569	$h \rightarrow l$
3	273.63	0.0230	$h \rightarrow l\text{+}1$	3	255.55	0.1169	$h \rightarrow l\text{+}1$
4	250.07	0.0332	*	4	244.37	0.0310	$h\text{-}1 \rightarrow l$

*Contribution of more than two transitions.

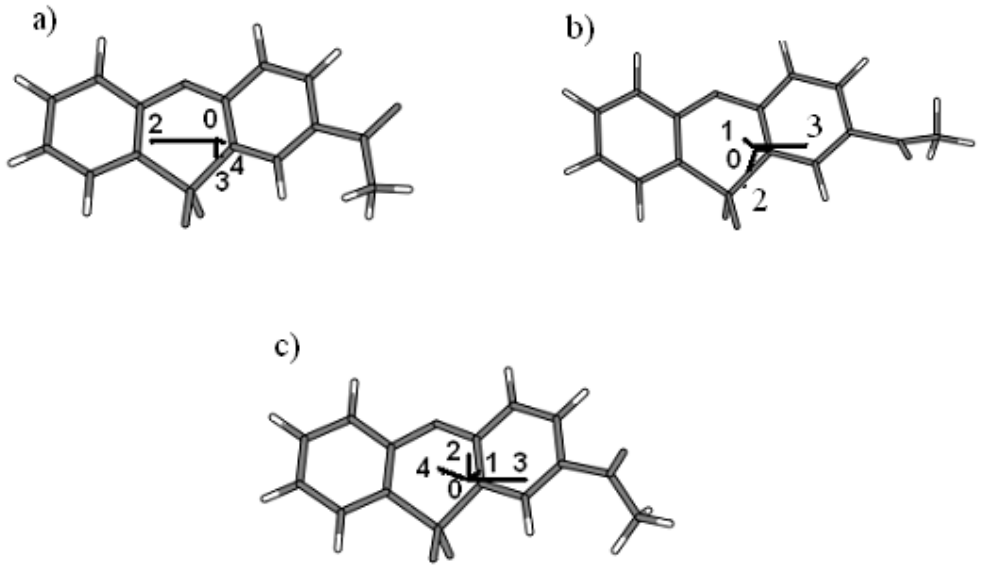

Fig. 33 Directions of the relevant transition moments (f > 0.0030) for the bands in the range of 230-350 nm for the conformers of Phx-SO_2-$COCH_3$: a) τ = 0° b) τ = 90° c) τ = 60°; 0 represents the origin of the molecular axes, and the numbers correspond to the transitions in Tab. 9.

The DFT calculations predict as more stable the planar conformations, the estimation of the barrier to rotation considering the difference between the energy for τ = 90° (maximum point on the potential energy surface built in respect to the torsion angle τ) and the energy for the minimum planar conformation (τ = 180°). The values are 6.93 kcal/mol and 6.42 kcal/mol for the B3LYP and PBE functionals, respectively.

Analysing the results for the two limit conformers, the planar and the twisted one (Tab. 9), it can be seen that the calculated spectra differ by the positions and the relative intensities of the bands.

Inspection of Fig. 33 shows that for the planar conformer, the moments corresponding to transitions 2 and 4 (289.51 nm and 250.07 nm) are polarized along the long molecular axis and transition 3 is polarized along the short molecular axis.

A comparison of the experimental ICD spectrum in the presence of β-CyD with the calculated electronic transitions for these two conformers shows that a parallel (axial) mode of inclusion is accounted for by the calculations.

The cavity of 2HP-β-CyD allows an axial inclusion mode, but determines also a selection of the included conformers, the conformers with τ around 60° being favoured.

In the case of α-CyD, the same ICD bands are observed but the sign is negative. We can therefore assume an orthogonal position of the guest in respect with the cavity axis; that corresponds better to a 1:2 ligand:α-CyD stoichiometry.

5.3 Theoretical modeling of inclusion complexes by molecular dynamics simulation

The molecular dynamics simulation of the 2:1 complex in water shows mainly a structure in which one of the cyclodextrins can be in a quasi-orthogonal orientation to the long axis of the ligand, Fig. 36.

a) b)

Fig. 36 Predominant of cyclodextrins in the inclusion complex of Phx-SO_2-$COCH_3$ with α-CyD in a trajectory of 1000 ps (water not shown).

5.4 CONCLUSIONS

The present results lead to the following conclusions. The binding constants of the cyclodextrin inclusion complexes of an achiral compound can be estimated with sufficient reliability using the experimental ICD data of the ligands for the cases in which the induced ellipticities are large enough, up to 8-10 mdeg.

For the ligands **Phx-SO_2** and **Phx-SO_2-CH_2Br**, ICD experimental spectra analysis shows that the stoichiometry of the inclusion complexes for β -, γ - and 2-HP-γ-CyD was 1:1 guest:host. The smaller interaction with α-CyD determines low induced chirality, preventing the estimation of the association constants. The substituent affects insignificantly the interaction process, the ICD spectra (positions of bands, alternation of signs) being similar. For both compounds, the larger association constants were obtained in the presence of β-CyD.

The theoretical calculations performed led to two main results. Firstly, the estimation of the energy barriers for the two processes, the butterfly motion of the heteroring and the rotation of the CH_2Br group, explains the achirality of the free guests, in spite of the possibility of some conformers, correlated with the bromine position in respect to the heteroring and the sulphone group, to present a significant rotational strength. Secondly, the chosen guests represent a favorable case for testing the TDDFT calculations as the polarizations of the electronic transitions are different and explain well the alternation of signs in the experimental ICD spectra. The directions of the calculated transition moments predict an axial inclusion way in the CyD cavity.

Our study shows that the circular dichroism spectroscopy represents a reliable and useful tool for studying the inclusion complexes in CyDs. The analysis of the ICD signals in the presence of CyDs allows the estimation of association constants and provides information on the inclusion mode in the cavity. The structural information obtained by correlating the experimental data with TDDFT calculations are a starting point in the modeling of the supramolecular guest:host system.

The interaction of 2HP-β-CyD with Phx-SO_2-CH_2Br allows an axial inclusion mode, but determines also a selection of the included conformers, the conformers with τ around 60^o being favoured.

In the case of the sistems Phx-SO_2:α-CyD and Phx-SO_2-CH_2Br:α-CyD, α-CyD, the same ICD bands are observed but the sign is negative. We can therefore assume an orthogonal position of the guest in respect with the cavity axis; that corresponds better to a 1:2 ligand:α-CyD stoichiometry.

In the **Phx-SO_2-$COCH_3$** interaction with CyD, the estimation of the binding constant was possible for β- and 2HP-β-CyD 1:1 complexes, but not for α-CyD. Binding constant for the Phx-SO_2-$COCH_3$:β-CyD system is in agreement with that obtained by fluorescence measurements (manuscript in preparation).

The correlation of the Harata and Kodaka empirical rules with TDDFT calculations provide a rational explanation for the differences between the induced signals in β-CyD and 2HP-β-CyD, considering that the asymmetry produced by the inclusion process is represented by the torsion of the acetyl group in respect with the π system of the heteroaromatic ring and by the preferential inclusion of different conformers, dependent on the cavity dimension. In the case of α-CyD, both the experimental and theoretical results support the formation of a complex with 1:2 ligand:cyclodextrin stoichiometry.

Our study shows that the circular dichroism spectroscopy represents a reliable and useful tool for studying the inclusion complexes in CyDs. The analysis of the ICD signals in the presence of CyDs allows the estimation of association constants and provides information on the inclusion mode in the cavity. The structural information obtained by correlating the experimental data with TDDFT calculations are a starting point in the modeling of the supramolecular guest:host system.

The molecular dynamics simulation shows a 2:1 structure for the inclusion complex CyD:ligand, in which one of the cyclodextrins was in a position almost orthogonal to the long axis of the ligand, which can be an explanation for the ICD spectra of the α-CyD inclusion complexes, for which dichroic bands with a negative sign appear.

Chapter 6

THE STUDY OF THE LIGAND-CYCLODEXTRIN INTERACTION BY ISOTHERMAL TITRATION CALORIMETRY

In this chapter are presented the results of the study by isothermal titration calorimetry of the interaction of α-, β-, γ-cyclodextrins with a series of ligands.

10,10-dioxide-phenoxathiin (Phx-SO_2)

For the interaction of Phx-SO_2 with α-, β-, γ-CyD the fitting of experimental data was done by keeping fixed the stoichiometric parameter n. The results are shown in Tab. 11.

Tab. 11 Thermodynamic parameters of the interaction of $FxSO_2$ with α-, β-, γ-CyD at 25ºC

CyD	n^*	K (M^{-1})	ΔH ($cal \cdot mol^{-1}$)	ΔS ($cal \cdot mol^{-1} \cdot grad^{-1}$)	ΔG ($cal \cdot mol^{-1}$)
α	1	371±24.9	-4578±230.3	-3.59±0.78	-3502.78±39.73
β	1	357±24.1	-4708±240.2	-4.11±0.81	-3480.0±39.96
γ	1	250±20.6	-3215±219.3	0.189±0.75	-3269.07±48.78

* imposed stoechiometry.

The variation of thermodynamic parameters indicated that the inclusion arises spontaneously (ΔG <0), accompanied by release of heat (ΔH <0) and decreasing entropy (ΔS <0). The main binding forces of Phx-SO_2 with α- and β-CyD were, according to thermodynamic parameters (ΔH <0, ΔS <0 and ΔG <0), are hydrogen bonds and van`der Waals interactions. Decrease of entropy can be due to conformational changes and confinement of ligand in the CyD cavity. The binding constants decrease from α- to β- and γ-CyD. For γ-CyD, the binding process of Phx-SO_2 results in a lower variation of enthalpy compared to the other two CyD, and the entropy change is very small and positive, reflecting the interaction of Phx-SO_2 with the larger cavity of γ-CyD.

Atenolol (ATE)

The interaction of ATE with α-, β-, γ-CyD was studied at 25°C, for solutions in pure water and in buffer solutions of pH 4.5, 7.4 and 10. In Fig. 40 is depicted the fitting of experimental data for β-CD titration with ATE in pure water.

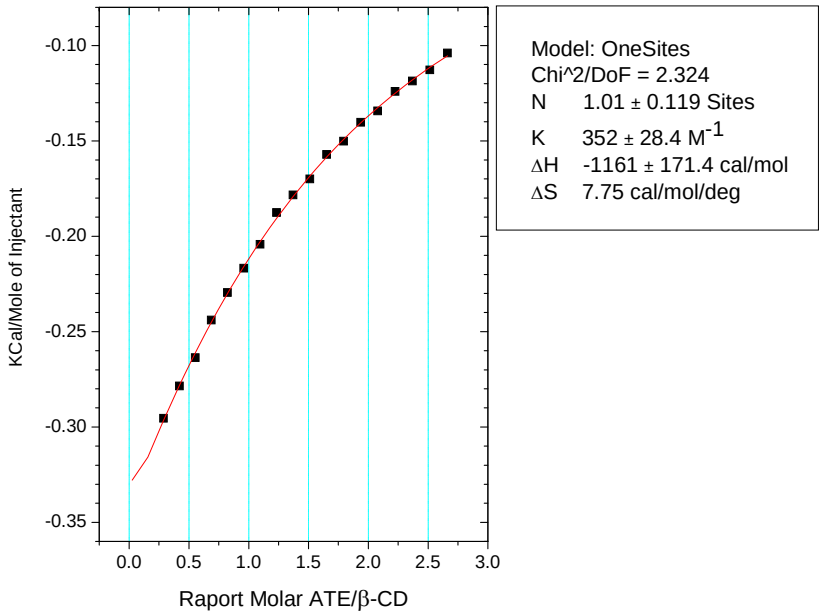

Fig. 40 The thermogram of titration of a solution 1.122×10^{-3} M β-CD with a 20.38×10^{-3} M ATE solution in pure water and the fitting of experimental data for a binding model to a single set of independent sites.

The measurements in solutions of pH buffer aimed at highlighting the interactions of the various species of atenolol with CyD. The variation of the thermodynamic quantities with the pH shows the influence of the environment on the predominant species involved in the interaction. Considering the value pKa = 9 of atenolol, it can be assumed that at pH = 10 the active species in solution is the deprotonated form. The results of fitting obtained for the calorimetric titration for the system β-CyD:atenolol in water and buffer solutions at pH = 4.5, 7 and 10 are given in Tab. 12. The thermal effect of ATE interaction with γ-CD in pure water was too small and could not be analyzed. For the titration of α- and γ-CyD with ATE in solutions at pH = 10, no thermal effect of the ATE-CyD interaction was revealed.

Tab. 12 The values of binding parameters for atenolol:β-CyD in different aqueous media obtained by fitting the experimental data

	pure water	pH=4.5	pH=7.4	pH=10
n	1.01±0.11	1*	1.47±0.28	1*
K (M^{-1})	352±28.4	222±25.9	263±44.5	294±11.6
ΔH (cal/mol)	-1161±171.4	-745.2±59.69	-824,5±213.2	-840.7±18.4
ΔS (cal/mol/deg)	7.75	8.24	8.31	8.48

* imposed parameter.

3-carboxy-5,6-benzocoumarin (BzCum)

For the BzCum interaction with β-CyD, the fitting of experimental data is shown in Fig. 44. The fitting was made to model sequential binding to two independent sites.

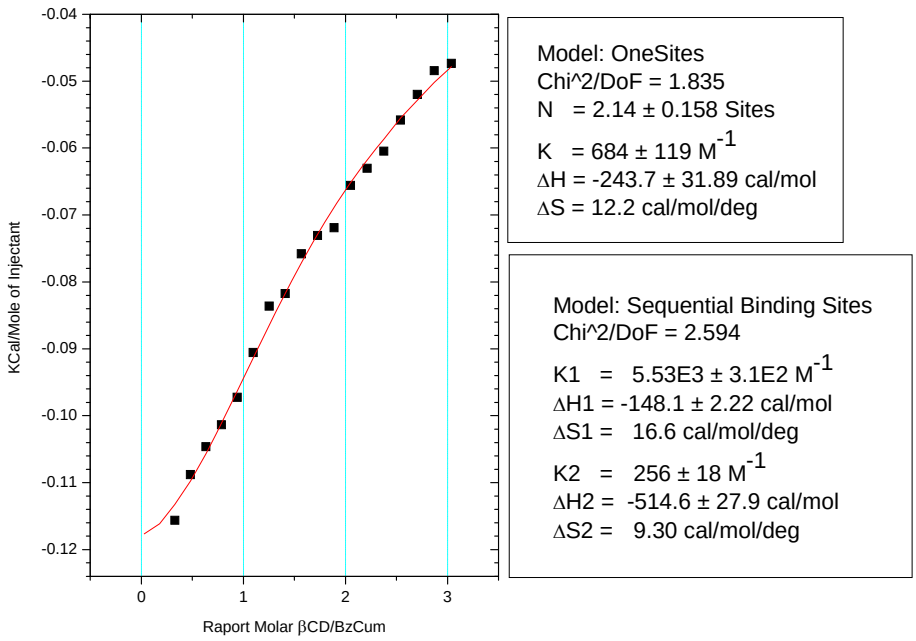

Fig. 44 The experimental data of the titration of $0.7055x10^{-3}$ M BzCum solution with a solution $1.59x10^{-2}$ M β-CD and the fitting of experimental data for the interaction of BzCum with β-CyD for the two binding models.

6.4 CONCLUSIONS

For the **FxSO$_2$** interaction with **α-**, **β-** and **γ-CyD**, the binding constants obtained ranged from 371±24.9 M^{-1} for the smallest cyclodextrin, to 250±20.6 M-1 for the largest cyclodextrin.

Since the binding constants of Phx-SO$_2$ with β- and γ-CyD were also determined by induced circular dichroism measurements, we find that for Phx-SO$_2$:β-CyD system, the constants obtained coincide, having the value of 357 ± 24.1 M^{-1}. For the Phx-SO$_2$:γ-CyD system, the binding constant obtained by circular dichroism was 223±17 M^{-1} as compared to the value of 250±20.6 M^{-1} obtained by calorimetry.

Concerning the interaction of **ATE** with **α-, β-** and **γ-CyD**, reliable data were only obtained for the interaction with β-CyD. The fitting results obtained for calorimetric titrations β-CyD-atenolol performed in water and buffer solutions with pH values of 4.5, 7 and 10 showed a 1:1 stoichiometry for the measurements performed in water and 1,4:1 at pH=7.4, the value of n being obtained by fitting without constraints. In other environments, the data obtained are less clear. Imposing the stoichiometry 1:1 for the inclusion complex, the experimental results have been fitted with the parameter statistics agreed, but with fitting without constraints, the results were not acceptable. Binding constants were from the lowest, 222 ± 25.9 M^{-1} at pH 4.5 to 352±28.4 M^{-1}, the highest in pure water.

In the case of **BzCum** interaction with **CyD**, calorimetric titration data reveals a 2:1 β-CyD:BzCum stoichiometry in OneSites fitting model, yielding an affinity constant K = 684±119 M^{-1}. For fitting experimental data, the model of sequential binding to two independent sites might be more plausible because of the two ends of the BzCum molecule, entering in one β-CyD cavity each, are not identical and, as a result, it is more natural to have two values of the binding constants that would illustrate this difference between the BzCum groups included in each β-CyD and also the interaction between the two cyclodextrins in the complex.

For **BzCum**, the interaction with **γ-CyD** resulted in a stoichiometry N=0.298±0.01, which means that a number of 3 molecules of BzCum interact with γ-CyD within either an inclusion or a non-inclusion complex. Thermodynamic parameters of interaction show an affinity constant K = 3.86E3±151 M^{-1} and the enthalpy and entropy changes ΔH = -8255±339.7 cal/mol and ΔS = -11.3 cal/mol/deg.

Chapter 7

THE STUDY OF THE LIGAND-ALBUMIN INTERACTIONS BY ISOTHERMAL TITRATION CALORIMETRY

In this chapter is presented the study by isothermal calorimetric titration of the interaction of some carboxylic derivatives of the coumarin class with human serum albumin.

7.2 MATERIALS AND METHODS

Materials

Fatty acid and globulin-free HSA was obtained from Sigma Chemical (St. Louis, MO, USA) The compounds 3-carboxy-5,6-benzocoumarinic acid and 3-carboxy-7-metoxycoumarinic acid were obtained from ABCR (Germany) and were used without further purification. The stock solution of phosphate buffer pH 7.4 was prepared using distilled and deionized water. The HSA, BzCum and MtCum solutions in buffer were prepared in pH 7.4 buffer.

7.3 RESULTS AND DISCUTIONS

3-carboxy-5,6-benzocoumarinic acid (BzCum)

The experimental results obtained for the interaction of BzCum with HSA using the two previously discussed calorimetric titration methods, the incremental and the single injection method, at 25ºC, are presented in Fig. 45.

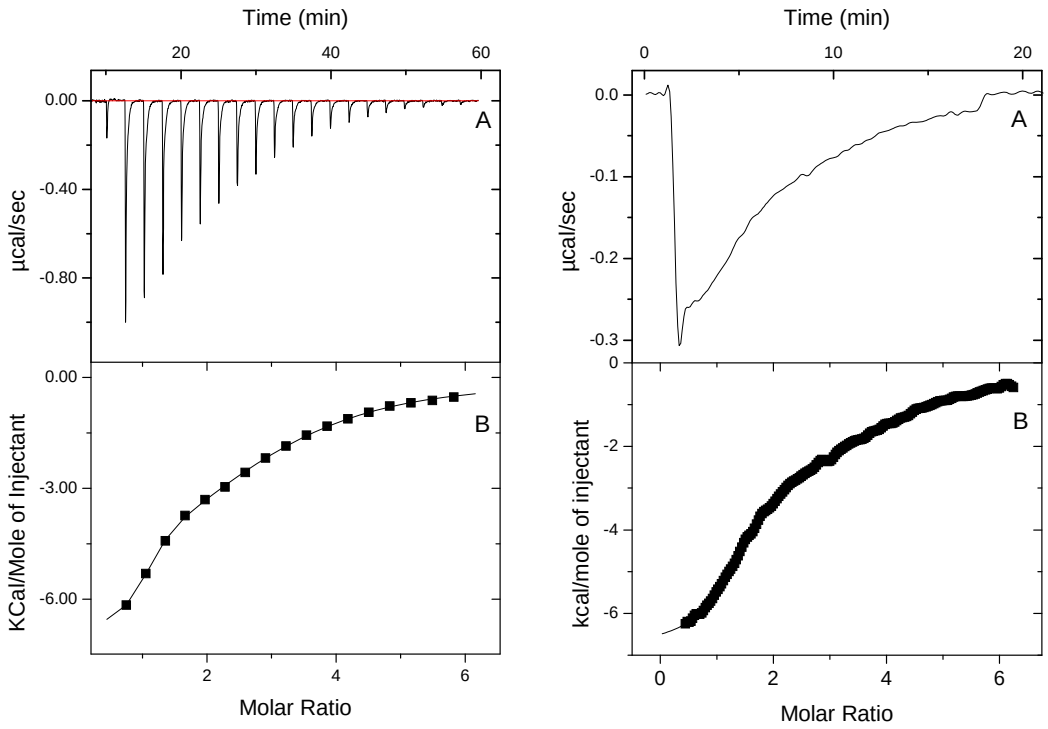

I **II**

Fig. 45 (A) Differential power (µcal/sec) versus time for titration of HSA with BzCum at 25ºC in phosphate buffer, pH 7.4, showing the calorimetric response as: I) successive injections of ligand are added to the reaction cell; II) continuous injections of ligand are added to the reaction cell. (B) Heat per injection from integration of the peak areas in part (A) per mole of injectant versus molar ratio. The continuous line represents the least-squares fit of the data to a two sets of sites binding model.

The best fit of the experimental ITC data was obtained for the two independent set of sites binding model, implemented in the Origin for ITC software. The results are listed in Tables 13 and 14.

Tab. 13 Thermodynamic parameters for the binding of BzCum to HSA from sequential ITC experiments

Temp ºC	n_1 Sites	K_1 (M^{-1})	ΔH_1 (cal·mol^{-1})	ΔS_1 (cal·mol^{-1}·grad^{-1})	ΔG_1 (cal·mol^{-1})	ΔC_{p1} (cal·mol^{-1}·grad^{-1})
15	0,82±0,02	2,54E6±5,15E5	-6890±231	5,39±0,89	-8438,74±116,01	
25	0,84±0,02	1,55E6±3,44E5	-7383±299	3,56±1,09	-8439,17±131,4	-89,7±23,3
35	0,85±0,04	5,25E5±9,63E4	-8684±337	-2,01±1,15	-8059,74±112,24	
Temp ºC	n_2 Sites	K_2 (M^{-1})	ΔH_2 (cal·mol^{-1})	ΔS_2 (cal·mol^{-1}·grad^{-1})	ΔG_2 (cal·mol^{-1})	ΔC_{p2} (cal·mol^{-1}·grad^{-1})
15	2,44±0,07	9,97E4±8,56E3	-3609±231	10,3±0,81	-6586,07±49,12	
25	2,67±0,13	5,87E4±5,88E3	-4125±376	7,98±1,27	-6501±59,3	-153,4±58,7
35	2,28±0,2	2,80E4±2,35E3	-6676±966	-1,32±3,13	-6266,07±51,35	

Tab. 14 Thermodynamic parameters for the binding of BzCum to HSA from continuous ITC experiments

Temp ºC	n_1 Sites	K_1 (M^{-1})	ΔH_1 (cal·mol^{-1})	ΔS_1 (cal·mol^{-1}·grad^{-1})	ΔG_1 (cal·mol^{-1})	ΔC_{p1} (cal·mol^{-1}·grad^{-1})
15	0,90±0,01	2,38E6±2,12E5	-6456±114	6,78±0,43	-8401,51±50,96	
25	0,76±0,02	1,59E6±4,14E4	-7028±306	4,80±1,03	-8454,25±15,41	-104,8±27,5
35	1,08±0,01	7,19E5±4,00E4	-8552±96,4	-0,95±0,33	-8252,17±34,04	
Temp ºC	n_2 Sites	K_2 (M^{-1})	ΔH_2 (cal·mol^{-1})	ΔS_2 (cal·mol^{-1}·grad^{-1})	ΔG_2 (cal·mol^{-1})	ΔC_{p2} (cal·mol^{-1}·grad^{-1})
15	2,15±0,04	8,03E4±3,38E3	-3414±130	10,6±0,46	-6462,24±24,08	
25	2,47±0,11	6,04E4±5,21E3	-4410±367	7,08±1,24	-6517,9±51,07	-161,15±35,5
35	2,34±0,09	2,80E4±1,16E3	-6637±413	-1,19±1,34	-6266,07±25,35	

The values of $\Delta H < 0$ and $\Delta S > 0$ at 15°C and 25°C show that both enthalpy and entropy contribute favorably to the binding process such that the interaction was enthalpy- and entropy-driven. According to the thermodynamic parameters (ΔH <0, ΔS >0 and ΔG <0), the main contributions on the binding forces in the BzCum-HSA system are provided by both hydrogen bonding and hydrophobic forces.

The binding free energy (ΔG), calculated as $\Delta G = -RT\ln K$, shows the compensation phenomena between the contributions of enthalpy and entropy changes as the temperature increases. Entropy decreases with temperature but the effect is compensated by the binding enthalpy (Fig. 47), the linear enthalpy–entropy relationship indicating the participation of water in ligand-protein binding processes [107].

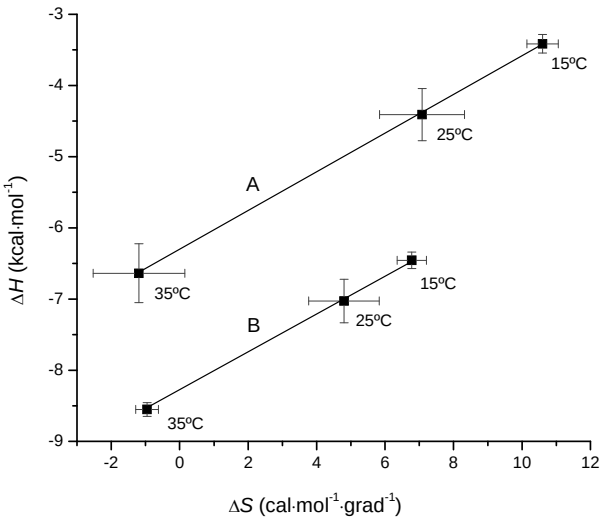

Fig. 47 Thermodynamic enthalpy-entropy compensation (values from Table 14) on temperature variation for: A. low-affinity sites and B. high-afinity site.

The dominant negative enthalpy suggests that there are a large number of favourable hydrogen bond contacts between the water of solvation released from hydrophobic surfaces and the water in bulk.

$\Delta Cp < 0$ usually correlated with the burial of hydrophobic surfaces. A negative ΔCp means that the net thermodynamic driving force for association will shift from being entropic to enthalpic with increasing temperature [108].

3-carboxy-7-metoxycoumarinic acid (MtCum)

For the MtCum interaction with HSA at 15, 25 and 35ºC, the results are presented in Tab. 15.

Tab. 15 Thermodynamic parameters for binding of MtCum to HSA from ITC data at temperatures 15, 25 and 35 ° C, for a three sequential binding sites model.

Temp ºC	Situsul Nr.	K_1 (M^{-1})	ΔH_1 (cal·mol^{-1})	ΔS_1 (cal·mol^{-1}·grad^{-1})	ΔG_1 (cal·mol^{-1})	ΔC_{p1} (cal·mol^{-1}·grad^{-1})
15	1	3,35E4±3,6E3	-1,672E4±1,22E3	-37,3±4,23	-5962,01±61,49	
25	1	4,49E4±6,1E3	-1,458E4±1,22E3	-27,6±4,1	-6342,32±80,43	162,5±29,7
35	1	4,92E4±1,8E3	-1,347E4±326	-22,3±1,06	-6611,01±22,38	
Temp ºC	Situsul Nr.	K_2 (M^{-1})	ΔH_2 (cal·mol^{-1})	ΔS_2 (cal·mol^{-1}·grad^{-1})	ΔG_2 (cal·mol^{-1})	ΔC_{p2} (cal·mol^{-1}·grad^{-1})
15	2	4,88E4±2,9E3	1,860E4±1,79E3	86,0±6,21	-6177,26±34,0	
25	2	2,90E4±4,4E3	1,711E4±1,83E3	77,8±6,14	-6083,51±89,83	407±148,95
35	2	2,87E4±1,7E3	1,046E4±539	54,3±1,75	-6281,18±36,24	
Temp ºC	Situsul Nr.	K_3 (M^{-1})	ΔH_3 (cal·mol^{-1})	ΔS_3 (cal·mol^{-1}·grad^{-1})	ΔG_3 (cal·mol^{-1})	ΔC_{p3} (cal·mol^{-1}·grad^{-1})
15	3	6,34E4±5,0E3	-1,136E4±695	-17,4±2,41	-6327,03±45,12	
25	3	4,79E4±3,6E3	-1,51E4±1,03E3	-29,5±3,46	-6380,62±71,69	-206,5±96,7
35	3	1,66E4±8,5E2	-1,549E4±284	-31,0±0,92	-5946,16±31,33	

7.4 CONCLUSIONS

The binding affinity of the 3-carboxy-5,6-benzocoumarinic acid (BzCum) to human serum albumin (HSA) was investigated at 7.4 pH, in phosphate buffer by isothermal titration calorimetry (ITC) at several temperatures, using both the stepwise and continuous titration method (cITC). From fitting the ITC data, it resulted that the BzCum binding occurs at two classes of independent binding sites. The first class contains a single high-affinity site, characterized by a binding constant of about $1.5x10^6$ M^{-1} at 25ºC. The second class is characterized by at least two sites with a binding constant of about $5.9x10^4$ M^{-1}. The binding was an exothermic process characterised by an enthalpy variation of about -7 Kcal mol^{-1} for the high-affinity site and about -4 Kcal mol^{-1} for the low-affinity sites. The heat capacity change (ΔCp) of binding was lower for the high-affinity site and negative for both sets of sites. The enthalpy and entropy dependence on temperature variation show that the interaction occured by enthalpy- and

entropy-driven mechanisms at 15°C and 25°C and became entirely enthalpy-driven at 35°C.

For the binding of MtCum to HSA, the best fittings of experimental data was for a sequential binding at three independent sites model. The MtCum binding affinities to HSA are of the order of the BzCum binding to HSA, at low affinity sites. Thus, at 25° C, the binding constants at the three sites have the values $4.95x10^4$, $2.51x10^4$ and $3.41 x10^4$ M^{-1} at the three sites, respectively. Binding was an exothermic process, characterized by a change of enthalpy of approximately -18 and -16 kcal mol^{-1} for the first and third site, respectively. For the second site, the binding was an endothermic process characterized by a change of enthalpy of about 18 kcal mol^{-1}. The entropy change was -41.4 and -34.3 $cal \cdot mol^{-1} \cdot grad^{-1}$ for the first and third situs and 83,3 $cal \cdot mol^{-1} \cdot grad^{-1}$ for the second site. The interaction was enthalpy determined for the first and third site and determined entirely entropic for the second site. The heat capacity variation was positive for the first and second site and negative for the third site.

GENERAL CONCLUSIONS

The thesis comprises a molecular interactions study in several supramolecular systems such as ligand-cyclodextrin and ligand-human serum albumin, with the aim of estimating thermodynamic parameters (stoichiometry, binding affinity, enthalpy and entropy) and structural features (inclusion mode in cyclodextrins and conformation changes after the binding process). The methods used were isothermal titration calorimetry and circular dichroism spectroscopy and the ligands were chosen to belong to different structural classes, namely coumarin derivatives, phenoxathiin derivatives and a cardiovascular drug, atenolol, a molecule with great flexibility.

The development of the objectives for this thesis has led to several conclusions for each system individually studied, conclusions analyzed at the end of the respective chapters. Tracking overall results allowed establishing the following general conclusions:

- The two methods used, the calorimetric method (isothermal titration calorimetry) and the spectral method (induced circular dichroism spectroscopy) have a totally different character and therefore may lead to different results in some cases.

- Thus, the main difference between the two methods is that the calorimetric method investigates the global thermal effect of all the processes that occur in the system during the ligand-macromolecule interaction, while the spectral method chosen, based on recording the induced circular dichroism spectrum, reflects only the effect of the surrounding environment found in the situs of the protein with maximum affinity for ligand or in the asymmetric cavity of cyclodextrins. Viewed from this perspective, the results can be seen as complementary. Although some systems in this thesis were addressed by both methods, because of small thermal effect recorded for some of them, we were unable to obtain a comparative image of these systems by the two methods. In the case of the interaction $FxSO_2$ with β- and γ-CyD, which could be studied by both methods, the results were similar in terms of stoichiometry and binding constant.
- The coupling of theoretical methods (DFT, TDDFT) with the analysis of experimental induced circular dichroism spectra in cyclodextrin-ligands systems allowed us to obtain information on the structure of the complex formed, on the inclusion mode in the cyclodextrin cavity and also to revealed the structural element that gives the ligand chirality, found in an asymmetric environment or in which the intramolecular movements are restricted.
- The correlation of the results of several experimental and theoretical methods with different character and, therefore, recording different aspects of molecular interactions, lead to a more complete picture of the ligand-cyclodextrin and ligand-protein supramolecular systems and is essential for a better understanding of molecular mechanisms of drug-receptor interactions.

LIST OF ARTICLES RESULTING FROM THE THESIS

Papers published

- Phenoxathiinsulphone derivatives–cyclodextrin interactions: Induced Chirality and TDDFT Calculations. Romică Sandu, Cristina Tăbleţ, Mihaela Hillebrand. *Journal of Inclusion Phenomena and Macrocyclic Chemistry*, (in press), available on-line, DOI 10.1007/s10847-012-0232-7.

- Binding affinity of the 3-carboxy-5,6-benzocoumarinic acid to human serum albumin: an isothermal titration calorimetry study. Romică Sandu, Mihaela Hillebrand, *Rev. Roum. Chim., 5, (2012*), *(in press).*

- Circular dichroism characterization of the inclusion complexes of 2-acetyl-phenoxathiin sulphone with cyclodextrines: experimental data and TDDFT calculations. Romică Sandu, Mihaela Hillebrand, *Rev. Roum. Chim., 56, 363-371*, *(2011)*.

Participation at conferences, posters

- Calorimetric study of interaction of some beta-blocker drugs with α-, β-, γ-cyclodextrins and human serum albumin, R. Sandu, C. Tăbleţ, V.T. Popa, S. Tanasescu, M. Hillebrand, Al 21-lea Simpozion anual de comunicări Ştiinţifice al Comisiei de Analiză Termică şi Calorimetrie, 17 Februarie 2012, Bucureşti.

- The use of the isotermal titration calorimetry method in analysis of the inclusion processes in cyclodextrins, R. Sandu, C. Tăbleţ, V.T. Popa, S. Tănăsescu, M. Hillebrand, Al 20-lea Simpozion anual de comunicări Ştiinţifice al Comisiei de Analiză Termică şi Calorimetrie, 11 Februarie 2011, Bucureşti.

- Investigation of the relationships between thermodynamics of binding interaction and therapeutical effects in drug delivery systems Iulia Contineanu, Ana Neacsu, Romică Sandu, Andreea Neacşu and Speranţa Tănăsescu, *ETP Nanomedicine General Assembly & Annual Forum, 14-15 October 2010, Milan, Italy*.

- Circular dichroism and fluorescence study of inclusion complexes of some phenoxathiine sulphones derivates with cyclodextrins*,* Romică Sandu, Mihaela Hillebrand, *13th International Conference on Physical Chemistry, 3-5 Sept. 2008, Bucharest, Romania,* (Poster).

- Thermodynamic properties of 3-formilphenoxathiin and β-cyclodextrin aqueous solution mixtures, Romică Sandu, Anca Sofronia, Tatiana Pascu, Mihaela

Hillebrand, *12th International Conference on Physical Chemistry, 6-8 Sept. 2006, Bucharest, Romania*, (Poster).

SELECTIVE BIBLIOGRAFY

1. A. Cooper, C. M. Johnson. Introduction to Microcalorimetry and Biomolecular Energetics in C. Jones, B. Mulloy and A. H. Thomas (Eds.), *Microscopy, Optical Spectroscopy, and Macroscopic Techniques.* Humana Press, Totowa, NJ, (**1994),** 109-124.

2. O'Brien R., Haq I., Applications of Biocalorimetry: Binding, Stability and Enzyme Kinetics; Biocalorimetry 2. by Ladbury J. E., Doyle M. L. (Eds). Wiley, UK, (**2004**), pp. 276.

9. R. Singh, N. Bharti, J. Madan, S. N. Hiremath, Journal of Pharmaceutical Science and Technology Vol. 2 (3), (**2010)**, 171-183.

10. H. Dodziuk, Cyclodextrins and Their Complexes: Chemistry, Analytical Methods, Applications, John Wiley & Sons, (**2006)**.

14. J. Szejtli, *Pure Appl. Chem.*, Vol. 76, No. 10, pp. 1825–1845, (**2004**).

16. Sudlow, G., Birkett, D. J. and Wade, D. N., *Mol. Pharmacol.* (**1975**), 11, 824-832.

17. Hiroshi Watanabe, Ulrich Kragh-Hansen, Sumio Tanase, Keisuke Nakajou, Maki Mitarai, Yasunori Iwao,Toru Maruyama, Masaki Otagiri, *Biochem. J.* (**2001**), 357, 269-274, 269.

18. Petitpas I, Bhattacharya A A, Twine S, et al. *J. Biol. Chem*. (**2001**), 276 (25): 22804—22809.

19. Patricia A Zunszain, Jamie Ghuman, Teruyuki Komatsu, Eishun Tsuchida, Stephen Curry. *BMC Structural Biology*, (**2003**), 3:6.

21. Matthew W. Freyer and Edwin A. Lewis*, Methods In Cell Biology,*(**2008),** Vol. 84

22. M. M. Pierce, C. S. Raman and B. T. Nall, *Methods.* (**1999**), 19, 213–221.

26. T. Wiseman, S. Williston, J. F. Brandts and L.-N. Lin, *Anal. Biochem.,* (**1989**), *179*, 131–137.

31. Richard K. Brown, J. Michael Brandts, Ronan O'Brien, William B. Peters. Label-Free Biosensors. (**2009**), pp 223-250.

33. S. Roselin, M-S. Lin, P-H. Lin, Y. Chang, W-Y. Chen, J. (**2010**), 5, 85–98.

40. Berova, N. (Ed.), Polavarapu, P.L. (Ed.), Nakanishi, K. (Ed.), R.W. Woody, R.W. (Ed.): Comprehensive Chiroptical Spectroscopy, Applications in Stereochemical Analysis of Synthetic Compounds, Natural Products, and Biomolecules**,** Wiley (**2012**).

41. Harata, K., Uedaira, H., Bull. Chem. Soc. Jpn. 48, 375–378, (**1975**).

42. Kodaka, M., J. Am. Chem. Soc. 115, 3702–3705, (1**993**).

43. Scott, R.L.: Some comments on the Benesi-Hildebrand equation. Rec. Trav. Chim., 75, 787-789 (**1956**).

44. Zsila, F., Bikadi, Z., Simonyi, M., Biochem. Pharmacol. 65, 447–456 (**2003**).

45. David C. Young, Computational Chemistry: *A Practical Guide for Applying Techniques to Real-World Problems*. (**2001**), John Wiley & Sons.

46. Runge, E.; Gross, E. K. U. Phys. Rev. Lett. (**1984**), 52, 997-1000.

47. Improta, R.; Barone, V.; Scalmani, G.; Frisch, M. J. J. Chem. Phys. (**2006**), 125, 54103-54112.

48. Luis Serrano-Andres, Manuela Merchan Journal of Molecular Structure: THEOCHEM, 729, (**2005**), 99–108.

49. Perdew J. P., Burke K., Ernzerhof, M. Phys. Rev. Lett. (**1996**), 77, 3865-3868; (**1997**), 78, 1396-1396.

50. Allouche, A.-R. , Journal of Computational Chemistry, 32, (**2011**), 174–182.

51. Hess B, Kutzner C, Van Der Spoel D, Lindahl E., *J Chem. Theory Comput.,* 4 (2): 435, (**2008**).

52.Yu, H., Rosen, M. K., Saccomano, N. A., Phillips, D., Volkmann, R. A., Schreiber, S. L., GROMACS Tutorial for Solvation Study of Spider Toxin Peptide.: Sequential assignment and structure determination of spider toxin omega-Aga-IVB. http://pdfdownloadfree.net/?pdfurl=1qeXpurpn6Wih-SUpOGumK6nh7PBxbK1q7iQu9fi5tXZ4sjg3ujelLza5OHb19XSl6jYpqCwh9qKoOOsnqKuiN3h2dyppZTr39yd4s7g59XjztGa5OPO19CT1dbenfLH4s7J1Z7c3OfYztTkyOLp2uTfk9zT3Iev5Q

53**.** Gromacs user manual. http://www.gromacs.org/@api/deki/files/152/=manual-4.5.4.pdf

54. Berendsen, H.J.C., Postma, J.P.M., van Gunsteren, W.F., Hermans, J., (**1981**). Intermolecular Forces, chapter Interaction models for water in relation to protein hydration, pp 331-342. Dordrecht: D. Reidel Publishing Company Dordrecht.

56. Gaussian 03, Frisch, M. J., Trucks, G. W., Schlegel, H. B., Scuseria, G. E., Rob, M. A., Cheeseman, J. R., Montgomery Jr., J. A., Vreven, T., Kudin, K. N., Burant, J. C.,

Millam, J. M., Iyengar, S. S., Tomasi, J., Barone, V., Mennucci, B., Cossi, M., Scalmani, G., Rega, N., Petersson, G. A., Nakatsuji, H., Hada, M., Ehara, M., Toyota, K., Fukuda, R., Hasegawa, J., Ishida, M., Nakajima, T., Honda, Y., Kitao, O., Nakai, H., Klene, M., Li, X., Knox, J. E., Hratchian, H. P., Cross, J. B., Bakken, V., Adamo, C., Jaramillo, J., Gomperts, R., Stratmann, R. E., Yazyev, O., Austin, A. J., Cammi, R., Pomelli, C., Ochterski, J. W., Ayala, P. Y., Morokuma, K., Voth, G. A., Salvador, P., Dannenberg, J. J., Zakrzewski, V. G., Dapprich, S., Daniels, A. D., Strain, M. C., Farkas, O., Malick, D. K., Rabuck, A. D., Raghavachari, K., Foresman, J. B., Ortiz, J. V., Cui, Q., Baboul, A. G., Clifford, S., Cioslowski, J., Stefanov, B. B., Liu, G., Liashenko, A., Piskorz, P., Komaromi, I, Martin, R. L., Fox, D. J., Keith, T., Al-Laham, M. A., Peng, C. Y., Nanayakkara, A., Challacombe, M., Gill, P. M. W., Johnson, B., Chen, W., Wong, M. W., Gonzalez, C., Pople, J. A.: Gaussian Inc., Pittsburgh, PA (**2003**).

57. Miehlich, B., Savin, A., Stoll, H., Preuss, H., Chem. Phys. Lett. 157, 200-206 (**1989**).

58. Perdew, P., Burke, K., Wang, Y. Phys. Rev. B 54, 16533-16539, (**1996**).

59. Perdew, J.P., Burke, K., Ernzerhof, M., Phys. Rev. Lett. 77, 3865-3868, (**1996**).

60. Tomasi, J., Mennucci, B., Cammi, R., Chem. Rev., 105, 2999-3093, (**2005**).

72. l. Birla, A. M. Cristian, D. Gavriliu, O. Maior and M. Hillebrand, *Rev. Roum.Chim*., (**2002**), *47*, 769-775.

73. A. Varlan and M. Hillebrand, *Molecules*, (**2010**), *15*, 3905-3919.

74. A. Varlan and M. Hillebrand, *Cent. Eur. J. Chem.*, (**2011**), *9*, 624-634.

75. A. Varlan and M. Hillebrand, *Rev. Roum. Chim.*, (**2010**), *55*, 69–77.

76. C. Stoica, A. Jelea and M. Hillebrand, *J. Photochem. Photobiol. A: Chemistry,* (**2006**), *183*, 89-97.

85. Hillebrand, M., Maior, O., Sahini, V.E., Volanschi, E.: Spectral study of some phenoxathiin derivatives and their positive ions. J. Chem. Soc. B, 755–761, (**1969**).

86. Ciureanu, M., Hillebrand, M., Volanschi, E.: ESR, Optical and Cyclic Voltammetric Study of the Electrochemical Reduction of Dibenz[b,e]thiepinone-5,5-dioxides. J. Electroanal. Chem. 322, 221–232, (**1992**).

87. Constantinescu, E., Hillebrand, M., Volanschi, E., Andrei, M., Ivanescu, G., Maior, O.: Cyclic voltammetry, ESR and spectral investigation of the electrochemical

reduction of some acethyl diphenyl sulphides and sulphones. J. Electroanal. Chem. 395, 211–220, (**1995**).

88. Ionescu, S., Gavriliu, D., Maior, O., Hillebrand, M.: Excited states properties of some phenoxathiin derivatives. J. Photochem. Photobiol. A 124, 67–73, (**1999**).

89. Preda, L., Lazarescu, V., Hillebrand, M., Volanschi, E.: Reactivity of substituted seven-membered heterocyclic sulfones: spectroelectrochemical study and theoretical modeling. Electrochim. Acta 51, 5587–5595, (**2006**).

90. Volanschi, E., Suh, S-H, Hillebrand, M.: Theoretical study on the reduction behaviour of sulphur containing heterocycles. I cleavage reaction of the C-S bond in the dibenzo[b,e]thiepinonesulphone class. J. Electroanal. Chem. 602, 181–188, (**2007**).

91. Ionescu, S., Gavriliu, D., Maior, O., Hillebrand, M.: Excited States Properties of some Phenoxathiin Derivatives, J. Photochem. Photobiol. A: Chemistry 124, 67–73, (**1999**).

92. Gad El-karim, I.A., J. Mol. Struct: THEOCHEM 945, 17–22, (**2010**).

93. Oana, M., Tintaru, A., Gavriliu, D., Maior, O., Hillebrand, M.: Spectral study and molecular modeling of the inclusion complexes of β--cyclodextrin with some phenoxathiin derivatives. J. Phys. Chem. B 106, 257–263 (**2002**).

94. Sandu, R., Hillebrand, M.: Circular dichroism characterisation of the inclusion complexes of 2-acetyl-phenoxathiin sulphone with cyclodextrins: experimental data and TDDFT calculations. Rev. Roum. Chim. 56, 363–371 (**2011**).

95. Vasiliu G., Maior, O: Chimia fenoxatiinei. Anal. Univ. Buc., 103-111 (**1964**).

100. R.L. Scott, *Rec. Trav. Chim.,* (**1956**), *75*, 787.

101. F. Barbato, B. Cappello, M.I. La Rotonda, A. Miro and F.Quaglia, *J. Incl. Phenom. Macrocycl. Chem.*, (**2003**), *46*, 179-185.

102. Y. Liu, B. Li, T. Wada and Y. Inoue, *Tetrahedron*, (**2001**), *57*, 7153-7161.

103. Y. Takenaka, H. Nakashima and N. Yoshida, *J. Mol.Struct.*, (**2007**), *871*, 149-155.

104. J.W. Park, H.E. Song and S.Y. Lee, *J. Phys. Chem B*, (**2002**), *106*, 7186-7192

105. ITC Data Analysis in Origin. Tutorial Guide Version 7.0, January (**2004**), MicroCal Inc., Northampton, MA, USA.

107. R. Lumry, and S. Rajender, *Biopolymers*, (**1970**), *9*, 1125–1227.

108. R. Talhout, A. Villa, A. E. Mark and J. B. F. N. Engberts, *J. Am. Chem. Soc*., (**2003**), *125*, 10570-10579.